Paper No. 376. (quote when citing this article)
Eleventh World Conference on Earthquake Engineering
ISBN: 0 08 042822 3

PREDICTION OF LIQUEFACTION-INDUCED LATERAL SPREADING BY DILATANT SLIDING BLOCK MODEL CALIBRATED BY CENTRIFUGE TESTS

V. M. TABOADA, T. ABDOUN, R. DOBRY

Civil Engineering Department, Rensselaer Polytechnic Institute,
Troy, NY 12180-3590
USA

ABSTRACT

Centrifuge model tests with in-flight shaking of liquefaction-induced lateral spreading indicate that the liquefied soil tries to dilate at large cyclic strains during the accumulation of deformation downslope. This dilative event results in a pore pressure dip, a regain in stiffness and strength for the soil, a high upslope acceleration spike, and a reduced lateral deformation D_H at the end of the shaking. As a result, the usual sliding block model, which does not consider this effect, overpredicts D_H at large earthquake accelerations, low shaking frequencies and steep slope angles. A modified dilatant sliding block model is calibrated by the centrifuge tests, with excellent agreement both in the values predicted for D_H and in the trends of variation of D_H versus acceleration, frequency and slope angle.

KEYWORDS

Liquefaction, geotechnical centrifuge, infinite slopes, lateral spreading, dilative behavior.

INTRODUCTION

Lateral spreading of mildly sloping ground is one of the most pervasive and costly types of liquefaction-induced ground failure. It destroys buildings, bridges, embankments and buried lifelines. In the 1906 San Francisco earthquake it was a major contributor to damage including severance of water lines and consequent hampering of firefighting efforts after the earthquake. More than 250 bridges were damaged in the 1964 Alaska earthquake by lateral spreading with a cost of several hundred million (in 1994 U.S. dollars). A significant fraction of the more than $1 billion dollars damage caused by the 1964 Niigata earthquake in Japan can be attributed to widespread lateral spreading. Significant lateral spread damage keeps recurring in major earthquakes, including the 1971 San Fernando and 1989 Loma Prieta events in California, the 1983 Nihonkai-Chubu earthquake in Japan, and the 1990 Philippines and 1991 Costa Rica earthquakes (NRC, 1985; Hamada et al., 1986; Bartlett and Youd, 1995; Ishihara, 1993). The recently 1995 Hyogo-Ken Nanbu earthquake in Kobe, Japan, was especially costly in that respect; it caused more than one hundred billion U.S. dollars in total damage, of which a significant fraction was related to liquefaction and lateral spreading effects.

Prediction of the lateral deformation, D_H, associated with lateral spreading is an involved engineering problem. Both complex numerical simulation codes and simplified engineering techniques have been proposed for this purpose. The simplified techniques can be broadly divided in three categories: (1) empirical

correlations between D_H measured in actual earthquake case histories and various soil, geometric and earthquake parameters (Hamada et al., 1986; Bartlett and Youd, 1995); (2) sliding block analysis of the lateral spread (Castro, 1987); and (3) other simplified techniques such as proposed by Towhata et al. (1991). The sliding block method was originally proposed by Whitman in 1953 (see Marcuson, 1994) and further developed by Newmark (1965) and Makdisi and Seed, (1978) for computing permanent deformations of dry and saturated dense sands and other stable soils in dams and embankments. Lately, it has become popular also for deformation analysis of liquefied soils, with a number of laboratory and field based procedures proposed to evaluate the yield or residual shear strength τ_y of the liquefied soil needed for the analysis (Castro, 1987; Seed and Harder, 1990; Ishihara, 1993; Baziar and Dobry, 1995). As discussed later herein, the sliding block model typically assumes that a mass of liquefied soil displaces downslope due to the upslope acceleration. The stress-strain behavior of the liquefied soil is assumed to be rigid-perfectly-plastic (or elastic-perfectly-plastic), with the key material parameter being the yield shear strength τ_y. This perfectly plastic soil response assumes that an unlimited soil deformation can be developed in each shaking cycle at constant shear stress τ_y. However, field and 1g and centrifuge shaking table observations have revealed that this is not true, and that in many or most liquefied sands there is an increase in strength of this liquefied soil at large cyclic strains due to its dilative response, with this strength increase playing an important role in limiting the value of D_H (Zeghal and Elgamal, 1994; Taboada, 1995; Dobry et al., 1995). Recently, Abdoun (1994) and Abdoun and Elgamal (1995) have modified the sliding block method to take into account this dilation effect in the prediction of D_H. In the rest of this paper, Abdoun and Elgamal's dilatant sliding block model is verified by means of centrifuge models of lateral spreading as well as relevant field information.

CENTRIFUGE RESULTS AND FIELD CORRELATION

Nine centrifuge models with in-flight shaking were tested in a laminar box to simulate the lateral spreading of an infinite slope of clean loose sand (Taboada, 1995). Figure 1 presents a sketch of the laminar box and instrumentation used. Each model consisted of a 20 cm high, uniform, clean, fine Nevada No. 120 sand layer, placed in the box at a relative density of 40% to 45%. It was fully saturated with water, inclined at an angle α to the horizontal, spun at a centrifuge acceleration of 50 g, and excited laterally at the base with an input acceleration time history consisting of 22 cycles of a 2 Hz prototype sinusoidal input, with variable amplitude, and maximum prototype peak acceleration ranging between 0.17 g and 0.46 g. In one of the tests, 22 cycles of f = 1 Hz instead of 2 Hz were used to verify the effect of frequency. Note that this acceleration time history is not horizontal, but also forms a slight angle α with the horizontal. Due mainly to the effect of the component of the weight of the rings parallel to the slope, and to the different hydrostatic pressures at both sides of the box caused by the water level being horizontal (Towhata, 1993), the prototype slope angle simulated in the field, α_{field}, is two to three times larger than α (Taboada, 1995). In the nine tests the value of α ranged from 0^o to 4^o, with the corresponding α_{field} ranging from 0^o to 10^o. For example, for $\alpha = 2^o$, $\alpha_{field} = 4.8^o$. That is, the model in Fig. 1, for the case $\alpha = 2^o$, simulates a fully submerged, infinite 4.8^o sand slope in the field having the material properties of the fine Nevada sand, except that it is 50 times more permeable (hence it is a coarse sand), subjected to shaking parallel to the slope.

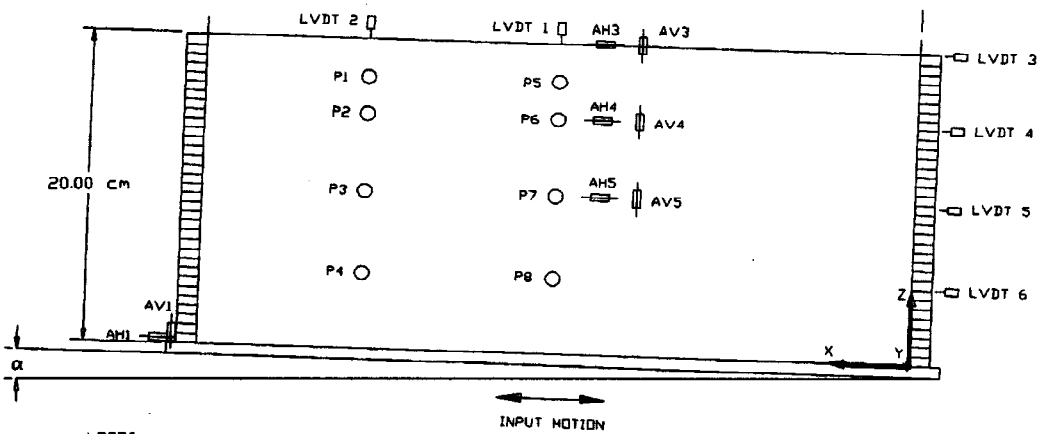

Fig. 1 Side view of RPI's laminar box and instrumentation (P-piezometer; AH-horizontal accelerometer).

The data points in Fig. 2 show the variation of the permanent prototype lateral displacement of the ground surface (D_H) measured by LVDT3, versus angle of prototype slope, α_{field}, obtained from seven centrifuge experiments of Nevada sand of the type sketched in Fig. 1. The input motion for all these tests was the same; the only parameter varied in the experiments was α_{field}, which ranged from 0^o to 10^o (Taboada, 1995). Superimposed on Fig. 2 is the curve obtained from the empirical correlation for lateral spreading free face case developed by Bartlett and Youd (1995), using multiple regression analyses on measured values of D_H in the field from a number of case histories. The constant 2.374 in the equation of this curve was obtained by normalizing Bartlett and Youd's empirical equation to the value $D_H = 46$ cm measured in the centrifuge at $\alpha_{field} = 4.8^o$. The curve and data points in Fig. 2 are in excellent agreement.

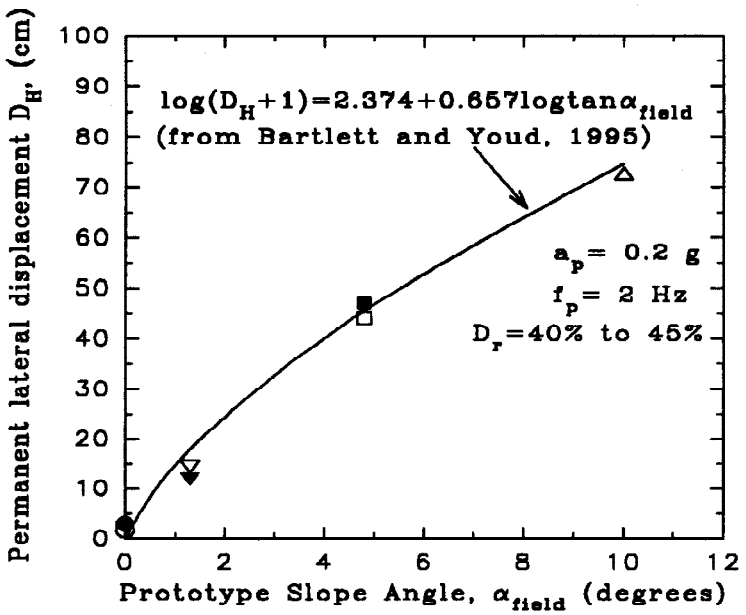

Fig. 2 Variation of D_H with angle of prototype slope measured in centrifuge model tests (data points), and predicted by Bartlett and Youd (1995) empirical correlation (curve). (For Bartlett and Youd's curve, $\tan\alpha_{field} = W/H$, and $D_H = 46$ cm for $\alpha_{field} = 4.8^o$, were used)

It was observed that the horizontal ($\alpha_{field} = 0^o$) and sloping ($\alpha_{field} > 1^o$) centrifuge models behave differently. In the horizontal model tests, after liquefaction, the accelerations in the liquefied soil were dramatically reduced, with the upper layers of the stratum becoming isolated from further seismic excitation. In the sloping tests, no reduction in acceleration was observed after liquefaction; instead, large upslope acceleration spikes and simultaneous drops in the piezometric records were recorded, which, as demonstrated by subsequent study, were due to the dilative shear-strain response of the saturated soil (Elgamal et al., 1996; Taboada, 1995). That is, the displacement in the downslope direction is arrested by dilatancy, which causes a sudden drop of pore pressure accompanied by deceleration which slows down and stops the movement of the mass. Figure 3a shows the spikes in the negative (upslope) direction recorded in one of the tests at a prototype depth of 2.4 m. The System Identification analysis originally developed by Zeghal and Elgamal (1994) to obtain the average shear stress-strain response of soil deposits in the field, was systematically applied to the lateral acceleration and displacement records obtained in these lateral spreading centrifuge tests. Figure 3b depicts the shear stress-strain response through the whole shaking for the liquefied soil in the same test. It must be noticed that the depth to liquefaction in this experiment was about 3.5 m. It may be observed that permanent deformations after liquefaction accumulated on a cycle by cycle basis, with a phase of shear regain in each cycle. This dilative response, which was observed to become stronger as the slope angle and input acceleration increased, and as input frequency decreased, limited the downslope strain accumulation and thus the value of the final lateral ground displacement. As mentioned before, similar acceleration spikes have been observed in the field and in other 1g and centrifuge shaking experiments, as well as in undrained cyclic tests of small specimens of Nevada sand (Arulmoli et al., 1992). In all nine tests, the lateral movements stopped as soon as the shaking ended, independently of the values of α, a_{max}, and f (Taboada, 1995).

SLIDING BLOCK ANALYSIS

The sliding block analysis (Newmark, 1965) has been used to represent seismically-induced stick-slip slope deformations for different sites/earth structures such as Heber Road site in Imperial Valley, California (Castro, 1987), and La Villita earth and rock fill dam in Mexico (Succarieh et al., 1993). A sliding block analysis assumes that the response of the moving soil mass can be represented by a sliding block over an inclined plane subjected to shaking (Fig. 4a).

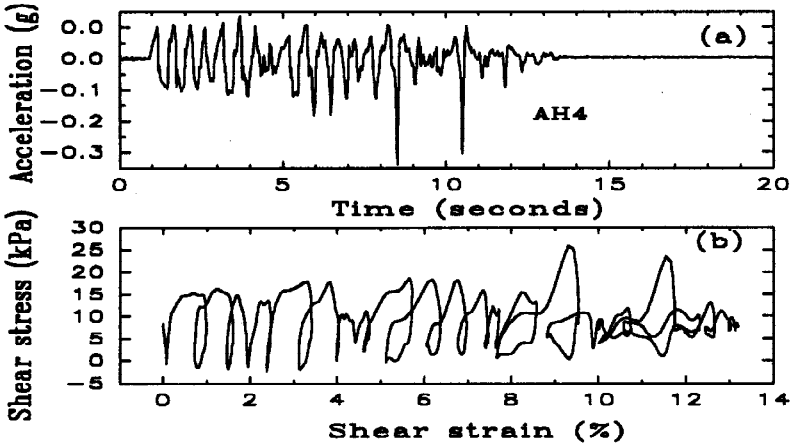

Fig. 3 Recorded response in Model No. 2: (a) lateral acceleration history recorded at 2.4 m depth and (b) shear stress-strain in the soil at a depth of 3.75 m.

The soil mass moves when the input ground acceleration exceeds the soil yield acceleration a_y defined by (Fig. 4a):

$$a_y = g \sin\theta \left(\frac{\tan\phi}{\tan\theta} \pm 1.0 \right) \tag{1}$$

where:

- g = acceleration of gravity
- a_y = yield acceleration
- θ = slope angle
- ϕ = soil angle of internal friction

In Eq. 1, the negative sign corresponds to downslope motion and the positive sign corresponds to upslope motion. The relative block velocity increases untill the ground acceleration falls below a_y (in absolute value). Thus, relative block velocity and displacement may be calculated by: i) integrating (over time) the acceleration histories of the slope and block, and ii) subtracting to obtain relative velocity and displacement histories. Following this logic, the relative block velocity v (in a given cycle) for a sinusoidal acceleration $a = A\sin(2\pi ft)$ is (simple case of yield in downslope direction only):

$$v = \frac{1}{2f\pi} \left(A\cos(2f\pi t_y) - A\cos(2f\pi t) + 2\pi f a_y (t_y - t) \right) \tag{2}$$

where:

- v = soil mass velocity (relative to the slope)
- f = ground acceleration frequency in Hz
- A = ground acceleration amplitude
- t_y = time at the start of yielding
- t = the time at the end of motion (substitute $v = 0$ in Eq. 2)

The corresponding induced relative block displacement (per cycle) can be calculated by integrating Eq. 2:

$$d = \frac{A\cos(2\pi f t_y)}{2\pi f}(t - t_y) - \frac{a_y}{2}(t_y - t)^2 + \frac{A}{4\pi^2 f^2}(\sin(2\pi f t_y) - \sin(2\pi f t)) \tag{3}$$

where:

d = permanent relative displacement per cycle

A similar approach may be used in the calculation of downslope-upslope yielding motion (Abdoun, 1994). The final lateral deformation for this type of motion is equal to the difference between uphill and downhill motions.

DILATIVE SLIDING BLOCK PHASE

A modification to the previous sliding block analysis is necessary to account for the increase in soil strength at large strains (due to dilation). If a_y and t_y are known, Eq. 2 may be used to calculate t. In first approximation, the induced displacement per cycle is given by Eq. 3, and the shear strain at the end of one cycle is assumed equal to the average value for the liquefied stratum:

$$\gamma = d / h \tag{4}$$

where, h = thickness of liquefied soil. If the amplitude of shear strain, γ_c, in any cycle is less than that necessary for dilation ($\gamma_c < \gamma_y$ as shown in Fig. 4b), no increase in strength occurs and the Newmark formulation applies in Eq. 3. The calculated time of motion and relative displacement do not need correction. On the other hand, if the shear strain induced in any cycle is greater than γ_y, a correction must be performed. In order to calculate the duration of motion and soil displacement during the soil strength-increase phase, a step by step integration procedure is used (Abdoun, 1994). The displacement accumulated before strength-increase, and the velocity are found from Eqs. 3 and 2, respectively (with $d_y = \gamma_y h$). In order to calculate the displacement during dilation, it is assumed that the soil shows an increase in shear strength $\Delta\tau$ (absolute value). Knowing the dilation slope m (Fig. 4b), one may calculate $\Delta\gamma$, and from Eq. 4 obtain Δd. The corresponding increase in yield acceleration may be defined as (Seed and Idriss, 1971):

$$a = \frac{\tau g^2}{\rho h} \tag{5}$$

with ρ = mass density of soil. Finally, the displacement increment is:

$$\Delta d = \Delta\gamma\, h = \int_{t_y}^{(t_y+\Delta t_n)} \Delta v\, dt = \int_{t_y}^{(t_y+\Delta t_n)} \int_{t_y}^{(t_y+\Delta t_n)} [A \sin(2\pi f t) - (a_y + \Delta a)]dt \tag{6}$$

Equation 6 may be used to calculate Δt in an iterative manner. The above steps are repeated untill the relative velocity reaches zero. The time increments Δt increase for a chosen constant change in shear strain ($\Delta\gamma$) since the soil mass relative velocity decreases with time. At the end of relative motion in this phase (v = 0), the total yielding time is:

$$t = t_y + \sum_{i=1}^{n} \Delta t_i \tag{7}$$

where, Δt_i = time increments during dilation, and n = number of increments. The total displacement is given by:

$$d = \gamma_y\, h + \Delta\gamma\, h\, n \tag{8}$$

The calculation procedure may be summarized in the following steps (Abdoun and Elgamal, 1996):
Step 1: Knowing the dilative shear strain γ_y (Fig. 4b), use Eq. 4 to calculate the corresponding dilative displacement d_y.
Step 2: Use Eq. 3 and Eq. 2 to calculate t_y and v_y, respectively, up to the beginning of dilation (with $d=d_y$).
Step 3: Assume an increase in the shear stress $\Delta\tau$, and use Eq. 5 to calculate the equivalent Δa. A very small increment of $\Delta\tau$ is used in order to maintain sufficient accuracy in reaching the state of $v = 0$.

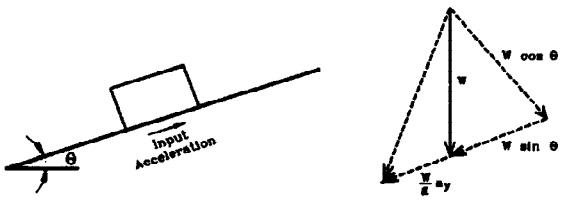

$$W \cos\theta \tan\theta = \frac{W}{g} a_y + W \sin\theta$$

a) Polygon of forces for a block on inclined plane

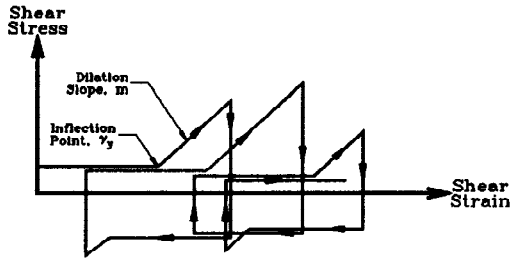

b) Simplified shear stress–strain relation (cycles of arbitrary amplitude with static shear stress offset)

Fig. 4 Sliding block on top of the ramp (slope) and shear stress-strain relation of the dilative sliding block.

Step 4: Knowing the dilation slope m, calculate $\Delta\gamma$. Use Eq. 4 to calculate Δd.
Step 5: By trial and error solve Eq. 6 to find Δt.
Step 6: Repeat steps 3-5, untill the relative velocity reaches zero (within the resolution dictated by $\Delta\tau$).
A computer program (Abdoun, 1994) was written to perform the above calculations, including the possibility of combined downslope-upslope yielding. The necessary input data may be summarized as: i) properties of the liquefied soil (cyclic strain to dilation γ_y, thickness of liquefied soil h, shear strength before dilation τ_y, and dilation slope m), ii) the equivalent dynamic input motion amplitude and frequency. In order to increase the versatility of the model, an additional computer program was written to calculate lateral deformation of sloping ground during earthquake shaking in the form of cycles of sinusoidal loading of arbitrary amplitudes.

MODEL PREDICTIONS AND COMPARISONS

The necessary input data were backfigured from the centrifuge results themselves, but were fixed for the nine experiments. The model predictions were performed on a liquefied soil layer of 3.5 m height in prototype, yield shear stress τ_y = 0.2 kPa, yield shear strain γ_y = 0.3 %, dilative slope m = 75°, and total unit weight = 2 t/m^2. The employed input acceleration in most of the tests was defined by A = 1.45 m/sec^2 with a frequency f = 2 Hz and N = 22 cycles. The 3.5 m layer of liquefied soil was obtained from pore pressure measurements in the centrifuge test. Figure 5 compares the permanent ground displacements D_H: (i) predicted by the sliding block model ($\gamma_y = \infty$), (ii) predicted by the modified dilative sliding block model (γ_y = 0.3 %), and (iii) measured in the centrifuge tests.

The variation of the measured permanent ground displacement D_H, with prototype slope angle α_{field}, is included in Fig. 5a. In the centrifuge experiments α_{field} was increased from 0° to 10°, while keeping the frequency and maximum amplitude of the input acceleration constant at 2 Hz and about 0.23 g, respectively. The centrifuge data in Fig. 5a are the same as Fig. 2. When the slope angle α_{field} increases, the soil mass tends to move downslope at a lower a_y and the final lateral deformation increases (Fig. 5a). A conventional sliding block analysis dictates that when the slope reaches about 6° the soil will yield indefinitely (driving static shear stress exceeds τ_y), which is unrealistic in view of the centrifuge observations. The dilative sliding block model, on the other hand, predicts that D_H will increase very slowly with further increases in the slope

angle at high values of α_{field}, which is in good agreement with the centrifuge measurements, as well as with the field observations (Fig. 2).

Figure 5b shows the variation of permanent ground displacement at the end of shaking, D_H, with input frequency for the case where $a_{max} \approx 0.20$ g, $\alpha_{field} \approx 5^o$, and number of cycles N = 22, as observed in three centrifuge experiments. The effect of input frequency predicted by the conventional sliding block analysis (no soil dilation) and the proposed dilative sliding block analysis are also shown in Fig 5b. At frequencies f > 4 Hz, both models predict the same displacement, since γ_c stays below γ_y =0.3 % in all cycles, and for the range 2 Hz < f < 4 Hz the predicted D_H are also similar in both cases. However, at lower frequencies f < 2 Hz, of common occurrence in large magnitude earthquakes, the predictions of the two models are extremely different, again with the dilative model agreeing much better with the centrifuge.

Figure 5c presents three centrifuge tests conducted using a prototype input acceleration frequency of 2 Hz and N = 22 cycles, where the slope angle α_{field} was about 5^o, and the input peak acceleration was increased from a_{max} = 0.23 g to a_{max} = 0.46 g. Again, the modified dilative sliding block model predicts the centrifuge measurements at high accelerations much better. In summary, examination of Fig. 5 indicates that in all cases involving development of large cyclic strains in the soil, due to either a steep slope angle, a low frequency or a high acceleration, the traditional sliding block model overpredicts D_H and exhibits the wrong trends. On the other hand, the modified dilative model predicts very well, both the trends and the values of D_H measured in the centrifuge tests.

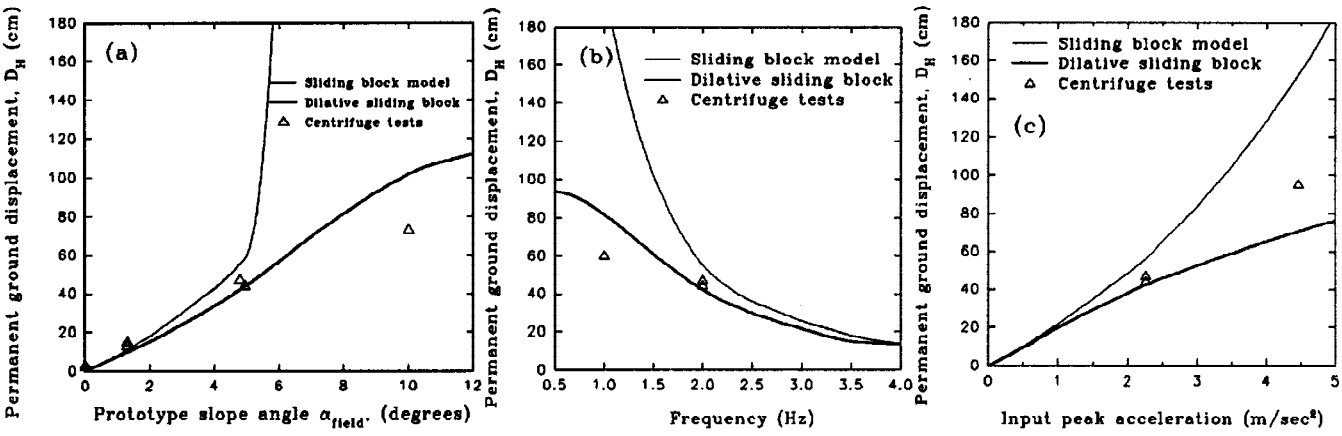

Fig. 5 Comparison of predicted and measured permanent ground displacements D_H versus: (a) slope angle, (b) input frequency, and (c) input peak acceleration.

CONCLUSIONS

The engineering method originally proposed by Abdoun and Elgamal (1996) for prediction of lateral deformation D_H due to lateral spreading of a uniform mass of saturated sand has been verified and calibrated by centrifuge model tests with in-flight shaking. This method is a modification of the well known sliding block model, now including a phase of strength regain for the liquefied soil at large strain excursions due to dilative response. The nine centrifuge tests revealed that the variation of D_H with slope angle, as well as shaking acceleration and frequency are well predicted by the proposed modified sliding block model. On the other hand, the original sliding block model without dilation significantly overpredicts D_H for step slopes, large accelerations and low frequencies.

ACKNOWLEDGMENTS

The authors want to thank Mr. Paul Van Laak for his help in conducting the centrifuge experiments. This work was supported by the Comisión Nacional de Ciencia y Tecnología de México (CONACYT), and by the

National Center of Earthquake Engineering Research (NCEER) and National Science Foundation (NSF) in the U.S.A. This support is gratefully acknowledged.

REFERENCES

Abdoun, T. H. (1994). Prediction of soil deformation due to seismically-induced liquefaction. Ms. Thesis, Dept. of Civil and Environmental Engineering, Rensselaer Polytechnic Institute, Troy, NY.

Abdoun, T. H., and A.-W. Elgamal (1996). Prediction of seismically-induced lateral deformation during soil liquefaction. ISSMFE, Intl. Regional Conf., Cairo, Egypt.

Arulmoli, K., K. K. Muraleetharan, M. M. Hossain, and L. S. Fruth (1992). VELACS: Verification of liquefaction analyses by centrifuge studies, laboratory testing program, soil data report, report, Earth Technology Corp., Irvine, CA, Project No. 90-0562.

Baziar, M. H. and Dobry., R. (1995). Residual strength and large-deformation potential of loose silty sands. *J. Geotechnical Eng.*, **121**, 896-906.

Bartlett, S. F., and T. L. Youd (1995). Empirical prediction of liquefaction-induced lateral spread, *J. Geotechnical Eng.*, **121**, 316-329.

Castro, G. (1987). On the behavior of soils during earthquake-liquefaction. Developments in geotechnical engineering 42, *Soil Dynamics and Liquefaction*, Cakmak, A. S., ed., Dept. of Civil Engineering, Princeton University, Princeton, NJ, pp. 169-204.

Dobry, R., Taboada, V. M., and Liu, L. (1995). Centrifuge modeling of liquefaction effects during earthquakes. *Proc. First Intl. Conference on Earthquake Geotechnical Engineering*, Tokyo, Japan, 14-16 November. Preprint volume of special, keynote and theme lectures, pp. 129-162.

Elgamal, A.-W., Zeghal, M., Taboada, V. M., and Dobry, R. (1996). Analysis of site liquefaction and lateral spreading using centrifuge testing records. Approved for publication in *Soils and Foundations*.

Hamada, M., Yasuda, S., Isoyama, R., and Emoto, K. (1986). Study on liquefaction induced permanent ground displacements. Association for the Development of Earthquake Prediction in Japan.

Ishihara, K. (1993). Liquefaction and flow failure during earthquakes. *Geotechnique* 43(3): 351-415.

Makdisi, F. I., and Seed, H. B. (1978). Simplified procedure for estimating dam and embankment earthquake-induced deformations., *J. Geotechnical Eng.*, **104**, 849-867.

Marcuson, W. F. (1994). An example of professional modesty. Proc., The Earth, Engineers and Education, A Symposium in Honor of Robert V. Whitman. MIT, Cambridge, Massachusetts, pp. 200-202.

National Research Council (NRC) (1985). Liquefaction of soils during earthquakes, Committee on Earthquake Engineering, National Research Council, Washington, D.C., *Rept. No. CETS-EE-001*.

Newmark, N. M. (1965). Effect of earthquakes on dams and embankments. *Geotechnique*, **5**.

Seed, H. B., and Idriss, I. M. (1971). Simplified procedure for evaluating soil liquefaction potential. *J. Soil Mechanics and Foundations Division*, **97**, 1249-1273.

Seed, R. B. and Harder, L. F. (1990). SPT-based analysis of cyclic pore pressure generation and undrained residual strength. *Proc., H. B. Seed Memorial Symp.*, BiTech Publishing, Vancouver, B. C., Canada, Vol. 2, 351-376.

Succarieh, M. F., A.-W. Elgamal and L. Yan (1993). Observed and predicted earthquake response of La Villita Dam. *Engineering Geology*, **34**, 11-26.

Taboada, V. M. (1995). Centrifuge modeling of earthquake-induced lateral spreading in sand using a laminar box. Ph. D. thesis, Civil Engineering Department, Rensselaer Polytechnic Institute, Troy, NY.

Towhata, I. (1993). Numerical predictions for Model No. 2. *Proc. of the Intl. Conf. on the Verification of Numerical Procedures for the Analysis of Soil Liquefaction Problems*. Arulanandan, K. and Scott, R. F. (eds.), Vol. 1, pp. 413-422. Rotterdam: Balkema.

Towhata, I., K. Tokida, Y. Tamari, H. Matsumoto, and K. Yamada (1991). Prediction of permanent lateral displacement of liquefied ground by means of variation principle. In T. D. O'Rourke and M. Hamada (eds), *Proc. Third Japan-U.S. Workshop on Earthquake Resistant Design of Lifeline Facilities and Countermeasures for Soil Liquefaction*, pp. 237-251, New York, NCEER, SUNY-Buffalo.

Zeghal, M., and A.-W. Elgamal (1994). Analysis of site liquefaction using earthquake records. *J. Geotechnical Eng.* **120**, 996-1017.